JACS
JOURNAL OF THE AMERICAN CHEMICAL SOCIETY
pubs.acs.org/JACS
Article

Radical SAM Enzyme HydE Generates Adenosylated Fe(I) Intermediates En Route to the [FeFe]-Hydrogenase Catalytic H-Cluster

Lizhi Tao, Scott A. Pattenaude, Sumedh Joshi, Tadhg P. Begley, Thomas B. Rauchfuss, and R. David Britt*

Cite This: *J. Am. Chem. Soc.* 2020, 142, 10841−10848
Read Online

ABSTRACT: The H-cluster of [FeFe]-hydrogenase consists of a $[4Fe-4S]_H$-subcluster linked by a cysteinyl bridge to a unique organometallic $[2Fe]_H$-subcluster assigned as the site of interconversion between protons and molecular hydrogen. This $[2Fe]_H$-subcluster is assembled by a set of Fe−S maturase enzymes HydG, HydE and HydF. Here we show that the HydG product $[Fe^{II}(Cys)(CO)_2(CN)]$ synthon is the substrate of the radical SAM enzyme HydE, with the generated 5′-deoxyadenosyl radical attacking the cysteine S to form a C5′−S bond concomitant with reduction of the central low-spin Fe(II) to the Fe(I) oxidation state. This leads to the cleavage of the cysteine C3−S bond, producing a mononuclear $[Fe^{I}(CO)_2(CN)S]$ species that serves as the precursor to the dinuclear Fe(I)Fe(I) center of the $[2Fe]_H$-subcluster. This work unveils the role played by HydE in the enzymatic assembly of the H-cluster and expands the scope of radical SAM enzyme chemistry.

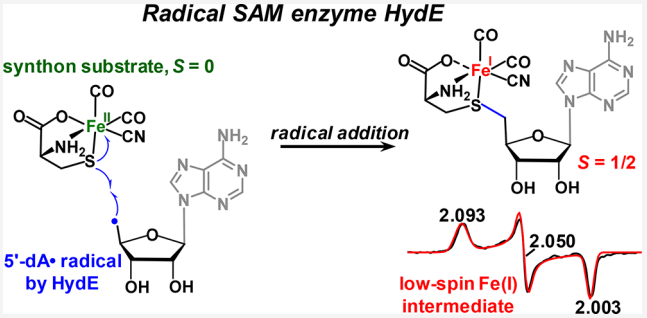

INTRODUCTION

The [FeFe]-hydrogenase enzyme, which efficiently catalyzes the reversible interconversion of H_2 and H^+/e^-, is important for microbial metabolism and serves as a model catalyst for the production and the use of hydrogen as a renewable fuel.[1] Its catalytic H-cluster (Figure 1) consists of a canonical $[4Fe-4S]_H$-subcluster linked to an organometallic $[2Fe]_H$-subcluster through a cysteine (Cys) residue.[2] There is much interest in understanding how nature biosynthesizes the $[2Fe]_H$-subcluster, in which the two Fe centers are coordinated by one bridging-azadithiolate ligand and multiple CO/CN^- ligands. Three Fe−S "maturase" enzymes, HydG, HydE, and HydF, play central roles in this biosynthesis.[3−5] The radical *S*-adenosyl-L-methionine (rSAM) enzyme HydG is currently the best understood: it lyses its substrate tyrosine using rSAM reactivity initiated at one 4Fe−4S cluster and then installs the resultant tyrosine-derived CO and CN^- onto a unique fifth "dangler" Fe of an auxiliary Fe−S cluster, ultimately forming its organometallic product, a $[Fe^{II}(Cys)(CO)_2(CN)]$ synthon which is vectored into the further synthesis of the $[2Fe]_H$-subcluster.[6−10] HydF has been proposed to serve as a scaffold in assembling the $[2Fe]_H$-subcluster and delivering it to the apo-hydrogenase.[11,12] Relatively little is actually known about the chemistry carried out by HydE, the other rSAM enzyme of the H-cluster maturase family. HydE has been hypothesized to play a role in building the bridging-azadithiolate ligand of the H-cluster, and assays of SAM turnover have been interpreted to favor a possible thiol-containing substrate.[13] In addition, Nicolet et al. have shown that HydE can react with the unnatural substrate 1,3-thiazolidine to form a new C5′−S bond.[14] Although this reaction has no direct biochemical significance to the generation of the H-cluster, it is relevant to the present report, where we have now identified a specific biosynthetic function for HydE in this important bioassembly process.

[FeFe]-hydrogenase can be produced via cell-free synthesis (or *in vitro* maturation, Figure 1) using the HydG, HydE, and HydF proteins delivered in their isolation lysates,[15] a cocktail of small molecule components along with an apo-hydrogenase HydA1 (*Chlamydomonas reinhardtii*) which is expressed with only the $[4Fe-4S]_H$-subcluster of the H-cluster.[15] In this process, HydG, the native source of the $[Fe^{II}(Cys)(CO)_2(CN)]$ synthon assembly precursor, is absolutely required for generating active hydrogenase enzyme. However, we have recently shown that the H-cluster in [FeFe]-hydrogenase can be installed through *in vitro* maturation

Received: April 7, 2020
Published: May 21, 2020

https://dx.doi.org/10.1021/jacs.0c03802
J. Am. Chem. Soc. 2020, 142, 10841−10848

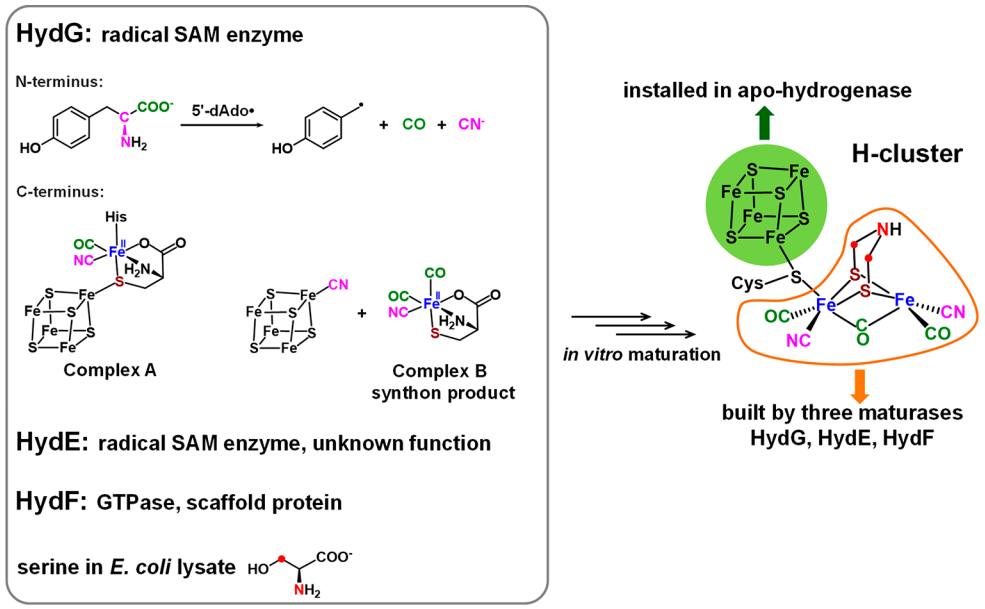

Figure 1. Cell-free in vitro maturation of [FeFe]-hydrogenase H-cluster requires three maturation enzymes: HydG, HydE, and HydF, in addition to the HydA1 apoenzyme that is expressed with only the [4Fe−4S] component. Alternatively, the H-cluster can be built by substituting the HydG enzyme with a synthetic synthon-complex "syn-B" that delivers the HydG-reaction product, a $[Fe^{II}(Cys)(CO)_2(CN)]$ synthon.[16] The colors displayed in the $[2Fe]_H$-subcluster correspond to the molecular sourcing, including the bridging-azadithiolate sulfurs (in burgundy) which come from the cysteine of the synthon,[16] and the C−N−C moiety (in red) which is sourced from serine (C3 and amino N).[17]

without the HydG enzyme, by instead including a synthetic "syn-B" complex in the maturation media.[16] On the basis of elemental analysis, syn-B appears to a cluster consisting of 3−4 $[Fe^{II}(Cys)(CO)_2(CN)(H_2O)]$ units bound to a high-spin Fe(II) center.[16] The key feature of syn-B complex is that it allows active hydrogenase maturation with only two maturase enzymes, HydE and HydF, i.e., it serves as a fully functional carrier of HydG's $[Fe^{II}(Cys)(CO)_2(CN)]$ product. This new semisynthesis route affords us the ability to initiate the *in vitro* maturation with isotopically labeled cysteine, or alternatively selenocysteine, synthetically preinstalled in the $[Fe^{II}(Cys)(CO)_2(CN)]$ synthon unit of syn-B.[16] This approach allows us to use pulse electron paramagnetic resonance (EPR) spectroscopy, extended X-ray absorption fine structure (EXAFS), and mass spectrometry to show that the two Fe-bridging sulfurs of the bridging-azadithiolate of the $[2Fe]_H$-subcluster are sourced from the cysteine sulfur of the synthon (or its selenium atoms if using selenocysteine).[16] However, the central C−N−C moiety of the bridging-azadithiolate is not supplied by this cysteine but is instead sourced from serine, specifically serine's C3 and the amino N.[17]

The isotope labeling, combined with isotope sensitive spectroscopy, has allowed us to determine the molecular sourcing of all the atoms of the H-cluster (Figure 1), but questions remain about the underlying enzymatic mechanisms for the steps beyond the HydG generation of the $[Fe^{II}(Cys)(CO)_2(CN)]$ synthon. How might the organometallic synthon be further tailored, and how might two such low-spin ferrous centers be brought together to make the binuclear cluster? To answer these questions one possible approach is to explore the reactivity of the HydG product synthon with the downstream maturation enzymes (HydE and/or HydF). While such attempts are largely impeded by the instability of the synthon product of HydG, we anticipate that employing the synthetic syn-B compound as a surrogate should facilitate our understanding of the later stages in the maturation pathway.

Herein, we report the reactivity of the rSAM enzyme HydE with selected isotopologs of the HydG product $[Fe^{II}(Cys)(CO)_2(CN)]$ unit as provided by the synthetic syn-B complex. We have identified that the role of rSAM enzyme HydE in the [FeFe]-hydrogenase H-cluster bioassembly is to enzymatically modify the HydG product $[Fe^{II}(Cys)(CO)_2(CN)]$ synthon by reducing the central Fe(II) to the Fe(I) oxidation state via a radical-addition mechanism that produces adenosylated Fe(I) intermediates. This reduction is followed by disassembling the Fe(I)-bound cysteinyl ligand to generate an $Fe^{I}S(CN)(CO)_2$ entity, which we propose serves as the precursor to the dinuclear Fe(I)Fe(I) center of $[2Fe]_H$-subcluster.

RESULTS

HydE contains a typical rSAM [4Fe−4S] cluster binding motif (CX_3CX_2C) near its N-terminus.[18−20] Such a [4Fe−4S] cluster is generally used to generate a highly reactive 5′-dA• radical via the reductive cleavage of a coordinated SAM. The canonical rSAM reaction employs this "hot" 5′-dA• radical to abstract an H atom from the enzyme's given substrate, such as the case of HydG where a hydrogen atom in the tyrosine amino group is abstracted as the first step in fragmenting tyrosine and generating CO and CN^-.[6,7,18,21] Some HydE enzymes, such as those from *Thermotoga maritima* and *Clostridium acetobutylicum*, also contain an accessory Fe−S cluster binding motif (CX_7CX_2C) at the C-terminus (Figure S1). However, this C-terminal cluster is not conserved (e.g., not present in *Shewanella oneidensis*, *Bacteroides thetaiotaomicron*, or *Desulfovibrio desulfuricans*)[22] and is not essential for the maturation of active [FeFe]-hydrogenase.[19]

To explore possible HydE reactivity with the synthetic $[Fe^{II}(Cys)(CO)_2(CN)]$ carrier, HydE-reaction mixture was prepared by mixing purified *Thermotoga maritima* HydE enzyme (*Tm*HydE, with its accessory cluster deleted by mutation as it has no reported function and provokes local structural heterogeneity),[14,19] along with the reductant sodium

https://dx.doi.org/10.1021/jacs.0c03802
J. Am. Chem. Soc. 2020, 142, 10841−10848

dithionite (DTH), SAM, and the syn-B complex. This reaction mixture was incubated for varying times before freeze-quenching in liquid nitrogen (*see* Methods). We then used EPR spectroscopy to detect and characterize any resulting paramagnetic intermediates.

Characterization of a 10 s Mononuclear Low-Spin Fe(I) Intermediate. As shown in Figure 2A, freeze-quenching

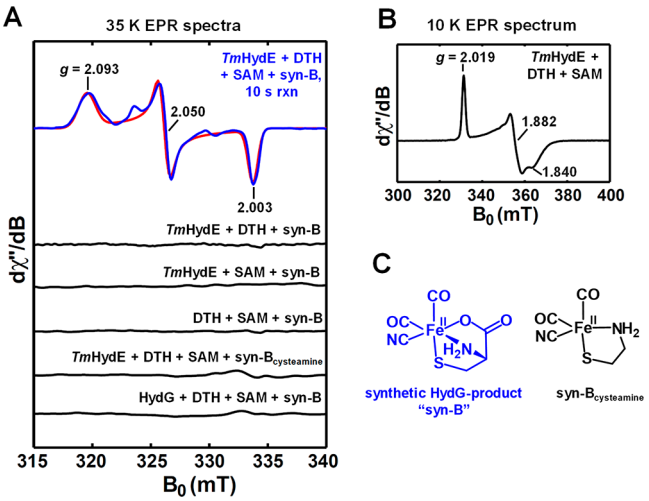

Figure 2. (A) X-band (9.37 GHz, 35 K) CW EPR spectrum (blue trace) of the *Tm*HydE reaction mixture prepared by incubating *Tm*HydE enzyme with 20 equiv of DTH, 10 equiv of SAM and 10 equiv of syn-B for 10 s before flash-freezing in liquid nitrogen. The red trace is a simulation using an $S = 1/2$ spin system and a **g** tensor of [2.093, 2.050, 2.003]. (B) X-band (9.37 GHz, 10 K) CW EPR spectrum of *Tm*HydE incubated with 20 equiv of DTH and 10 equiv of SAM. The spectrum shows only the SAM-bound $[4Fe{-}4S]^{+}_{RS}$ cluster in *Tm*HydE, which has a **g** tensor of [2.019, 1.882, 1.840]. (C) Depiction of the low-spin Fe(II) organometallic units supplied by syn-B and syn-B-cysteamine complexes.

after a time of 10 s produces a single paramagnetic species with an $S = 1/2$ rhombic EPR spectrum (35 K) with a **g** tensor of [2.093, 2.050, 2.003]. This signal is distinct from that of the reduced SAM-bound $[4Fe{-}4S]^{+}$ cluster (Figure 2B) of *Tm*HydE, which has a **g** tensor of [2.019, 1.882, 1.840], and which can only be detected at lower temperature (10 K) due to its intrinsic rapid spin-relaxation. Control experiments (Figure 2A) show that all four components, *Tm*HydE enzyme, DTH, SAM, and syn-B, are required for generating this novel paramagnetic species, indicating that syn-B is reacting with *Tm*HydE through a HydE-mediated rSAM reaction. Moreover, this reaction is both HydE and syn-B specific, as no paramagnetic intermediates are generated when we replaced *Tm*HydE with another rSAM enzyme, HydG, or when we employed another Fe(II) compound that carries a $[Fe^{II}(cysteamine)(CO)_2(CN)]$ unit instead of $[Fe^{II}(Cys)(CO)_2(CN)]$ (Figure 2C). Observation of this 10 s paramagnetic intermediate shows that the $[Fe^{II}(Cys)(CO)_2(CN)]$ synthon unit donated by syn-B is a functional substrate for the rSAM chemistry mediated by *Tm*HydE.

The rhombic **g** tensor for the 10 s-intermediate corresponds to an isotropic component $g_{iso} = 2.049$ ($g_{iso}^2 = (g_1^2 + g_2^2 + g_3^2)/3$), which deviates significantly from the value $g_e = 2.0023$ for a free electron. The *g*-value deviation, proportional to the one-electron spin–orbit coupling constant,[23] suggests that the 10 s-intermediate signal is metal-centered, presumably a species resulting from HydE's reaction with the $[Fe^{II}(Cys)(CO)_2(CN)]$ substrate. We can rule out an Fe(II) origin, which would be either low-spin diamagnetic ($S = 0$) or integer high-spin ($S = 2$) with a dramatically different EPR spectrum, likely unobservable in our conventional perpendicular-polarization X-band EPR measurement.[24] We considered a low-spin Fe(III) (3d,[5] $S = 1/2$) origin for the signal. However, due to the very significant spin–orbit coupling effects, low-spin Fe(III) species typically offer dramatically different **g** tensors with a much larger g_{max} ($\gtrsim 3.0$) and much broader overall spectral lineshapes.[23,25] These considerations indicate that the 10 s-intermediate is a low-spin Fe(I) (3d,[7] $S = 1/2$) species. The **g** tensor of this 10 s-intermediate is quite similar to that of the H_{ox} state of the H-cluster (*g*-values = [2.103, 2.042, 1.998]), in which the $[2Fe]_H$-subcluster is poised in a mixed-valence Fe(II)Fe(I) state with most of the spin density carried by the Fe(I) site distal to the $[4Fe{-}4S]_H$-subcluster.[26] Also, the 10 s-intermediate's **g** tensor is close to that of a synthetic low-spin mononuclear Fe(I) compound with a side-on acetylene ligand ($S = 1/2$, *g*-values = [2.114, 2.040, 2.007]).[27] Therefore, the EPR spectra and analyses suggest that the 10 s-intermediate corresponds to a low-spin Fe(I)-containing species resulting from a HydE mediated one-electron reduction of the Fe(II) center of the synthon unit.

To further probe the structure of the 10 s-intermediate, we generated its isotopologues using syn-B containing ^{13}CN or $^{13}C_3/^{15}N$-Cys ligands. Hyperfine couplings to these magnetic isotopes were probed using the pulse EPR technique of ENDOR (Electron Nuclear Double Resonance) (Figure 3). The Q-band ^{13}C Davies-ENDOR spectra of the 10 s-intermediate generated with syn-B–^{13}CN (Figure 3A) shows one set of strongly coupled ^{13}C with $A = [28.5, 22.0, 29.5]$ MHz, a hyperfine coupling comparable to the strongly coupled ^{13}C of ^{13}CN assigned to the distal Fe(I) center of the H_{ox} state of the H-cluster.[26] Also, the corresponding X-band CW EPR spectrum (Figure S2) shows a ^{13}C-split doublet at g_3, analogous to the splitting seen in the ^{13}CN-labeled H_{ox} state CW EPR signal.[26] In addition, only this strongly coupled ^{13}C is observed, and no weaker-coupled ^{13}C such as that assigned to the ^{13}CN of the proximal Fe(II) of the H-cluster can be detected (Figure S3). These ENDOR results further support our *g*-tensor based Fe(I) assignment to the 10 s-intermediate, and also suggest that it is an Fe(I) monomer since a mixed valence Fe(II)Fe(I) species similar to the $[2Fe]_H$-subcluster in the H_{ox} state would likely show a second ENDOR signal from a more weakly coupled ^{13}CN. This identification of the 10 s Fe(I) monomer intermediate confirms that the $[Fe^{II}(Cys)(CO)_2(CN)]$ synthon unit carried by syn-B is successfully delivered to the HydE enzyme and converted to a new species, revealing that the organometallic $[Fe^{II}(Cys)(CO)_2(CN)]$ synthon product of HydG is the substrate for HydE.

The $^{13}C_3/^{15}N$-Cys isotopologue of syn-B was used to examine if the cysteine ligand is also present in the 10 s-intermediate. Here two sets of ^{13}C hyperfine-couplings ($A = [1.05, 1.50, 1.38]$ MHz and $A = [0.42, 0.98, 0.96]$ MHz), as well as one set of ^{15}N couplings ($A = [5.41, 5.69, 4.23]$ MHz), are detected with Q-band pulse ENDOR spectroscopy (Figure 3B), demonstrating that the cysteine introduced in the $[Fe^{II}(Cys)(CO)_2(CN)]$ synthon unit remains as a ligand to the Fe(I) center of the 10 s-intermediate.

A striking result was obtained when the 10 s-intermediate was generated using $^{13}C_{10}$-adenosine-labeled SAM (Figure 3C). ENDOR experiments reveal a ^{13}C hyperfine coupling (*A*

https://dx.doi.org/10.1021/jacs.0c03802
J. Am. Chem. Soc. 2020, 142, 10841–10848

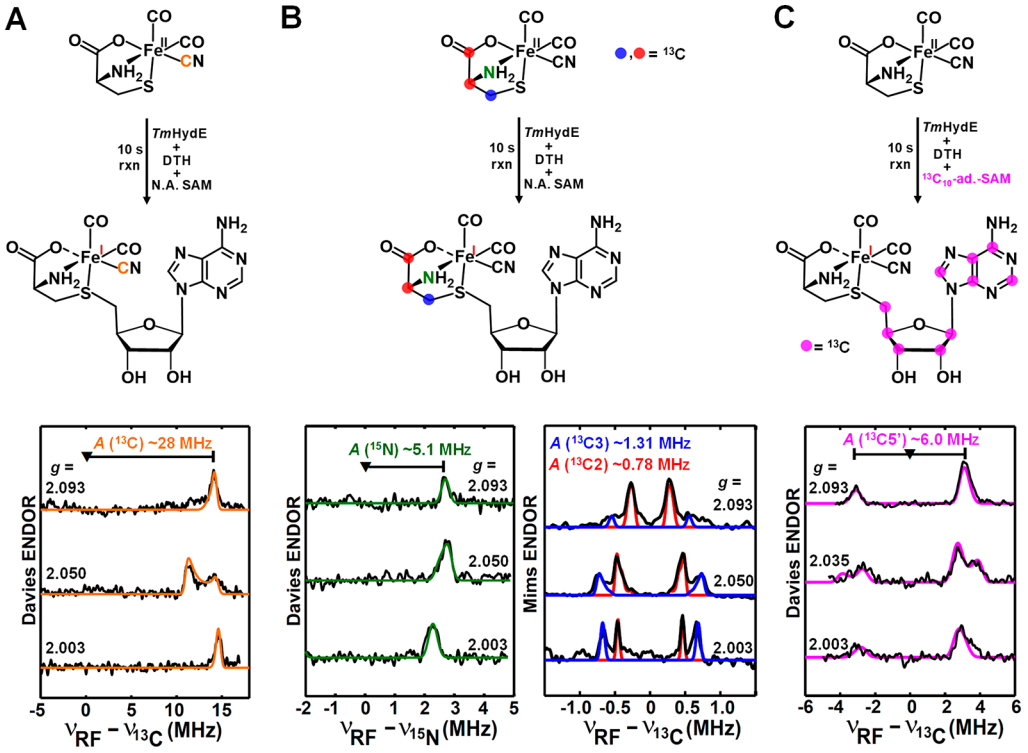

Figure 3. ENDOR spectra (15 K) and a proposed ENDOR-based structure of the 10 s-intermediate of *Tm*HydE reaction, using (A) syn-B−^{13}CN, (B) syn-B−$^{13}C_3$/^{15}N-Cys or (C) $^{13}C_{10}$-adenosine-labeled SAM. The ^{13}C hyperfine-coupling signals of ^{13}CN (**A**) and ^{13}C5′ (**C**), as well as the ^{15}N hyperfine-coupling signal (B, left panel) from $^{13}C_3$/^{15}N-Cys were detected by Q-band Davies- ENDOR with experimental parameters of: 34.06 GHz, microwave inversion pulse π = 80 ns, $\pi/2$ = 12 ns, τ = 300 ns, and RF pulse = 20 μs. The two sets of ^{13}C hyperfine-coupling signals from $^{13}C_3$/^{15}N-Cys (B, right panel) were detected by Q-band Mims-ENDOR with experimental parameters as 34.04 GHz, $\pi/2$ = 12 ns, τ = 300 ns, and RF pulse = 20 μs. All experimental spectra are in black, and the simulated spectrum are in color representing the labeled isotopes. The simulation parameters are given in the SI.

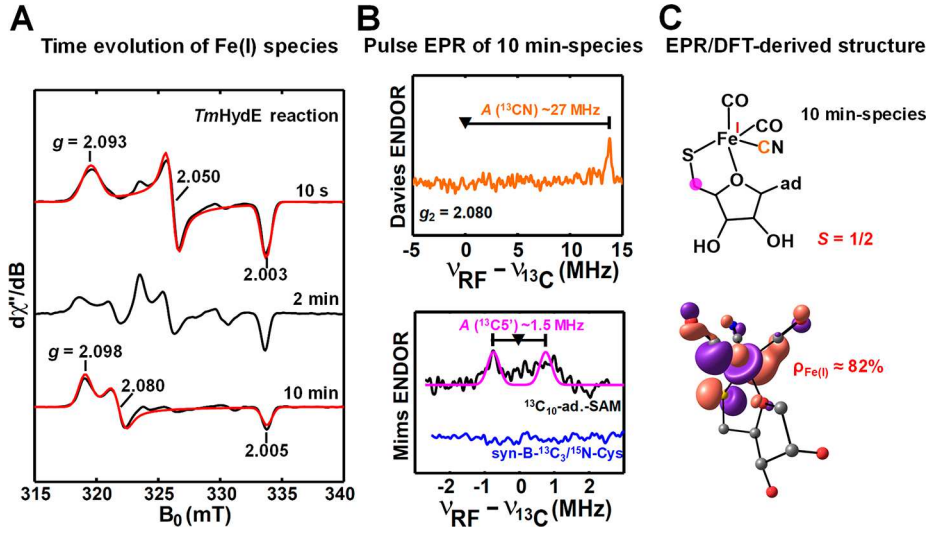

Figure 4. (A) X-band (9.37 GHz, 35 K) CW EPR spectra (black) of *Tm*HydE reaction mixtures freeze quenched at 10 s, 2 min, or 10 min. The top red trace is the simulation using an S = 1/2 spin system and a **g** tensor of [2.093, 2.050, 2.003]. The bottom red trace is the simulation using an S = 1/2 spin system and a **g** tensor of [2.098, 2.080, 2.005]. The analysis of the more complicated 2 min-spectrum is provided in Figure S7. (B) Q-band Davies- and Mims- ENDOR spectra of the isotopically labeled 10 min-species of *Tm*HydE reaction by syn-B−^{13}CN (orange trace), syn-B−$^{13}C_3$/^{15}N-Cys (blue trace) or $^{13}C_{10}$-adenosine-labeled SAM (experimental spectrum in black and the simulated spectrum in magenta). (C) The proposed structure of the 10 min-species based on EPR/ENDOR data. DFT calculated SOMO (singly occupied molecular orbital) of the 10 min-species is shown with isosurface value 0.05 au (see Figure S8 for details).

= [6.0, 4.8, 8.2] MHz) between the Fe(I) spin-center and one ^{13}C of the $^{13}C_{10}$-adenosine-labeled SAM, indicating a linkage between the Fe(I) center and the adenosine moiety of SAM. This ^{13}C coupling is stronger than the ^{13}C couplings from the cysteine ligated via amino and thiol groups but weaker than that of the directly coordinated ^{13}CN. The ^{13}C coupling is also

https://dx.doi.org/10.1021/jacs.0c03802
J. Am. Chem. Soc. 2020, 142, 10841−10848

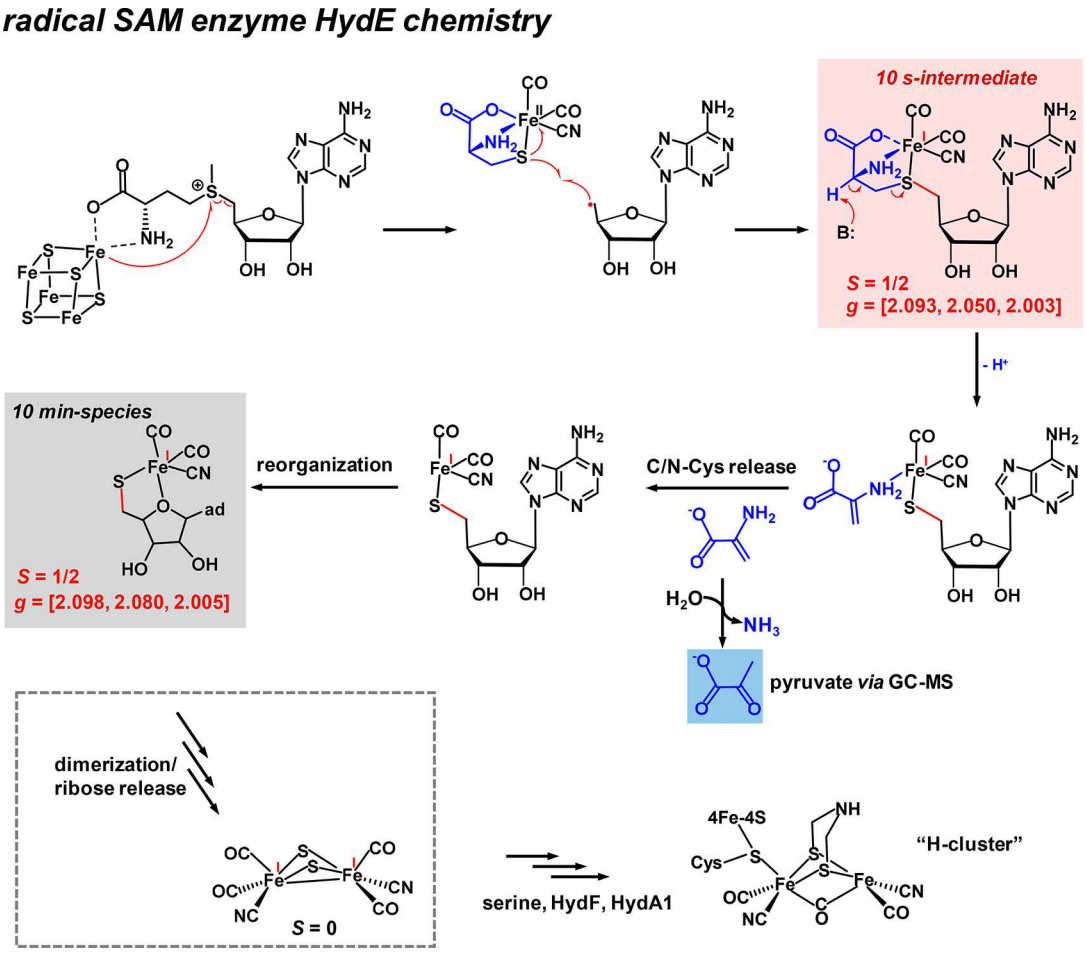

Figure 5. Overview of our proposed reaction pathway of HydE reacting with the HydG product[Fe^{II}(Cys)$(CO)_2$(CN)] synthon. The Fe(I)Fe(I) dimer species shown following the 10 min-species (within the dashed box) is currently speculative.

weaker than that reported for the "Omega" organometallic intermediate where the C5′ of adenosine is directly coordinated to an Fe of the 4Fe−4S cluster.[28] Theoretical calculations (see DFT results in Figures S4 and S5) suggest this ∼6.0 MHz ^{13}C coupling reasonably arises from the C5′ covalently linked to the Cys sulfur atom, as shown in Figure 3C, and as precedented by the prior study that shows the 5′-dA● radical generated by *Tm*HydE directly attacks the sulfur atom of an unnatural substrate, 1,3-thiazolidine, forming a new C5′−S bond.[14]

In this case with syn-B providing the [Fe^{II}(Cys)$(CO)_2$(CN)] synthon, such a linkage would be possible if the 5′-dA● attacks the electron-rich sulfur atom of Cys in [Fe^{II}(Cys)$(CO)_2$(CN)] to form a new C5′−S bond. Radical addition to sulfur would be accompanied by the one-electron reduction of the Fe(II) center to Fe(I), consistent with the collective results described above (Figure 5). To confirm this proposal we turned to high-performance liquid chromatography−mass spectrometry. While it was not possible to detect the fully intact 10 s organometallic intermediate, we succeeded in detecting the proposed organic *S*-adenosyl-L-cysteine adduct, with appropriate mass patterns found in reactions carried out using $^{13}C_{10}$-adenosine-labeled SAM, syn-B−$^{13}C_3$/^{15}N-Cys or syn-B-selenocysteine (Figure S6). These results confirm the presence of the *S*-adenosyl-L-cysteine moiety and reinforce our proposed mechanism invoking 5′-dA● radical addition to cysteine sulfur.

These results establish the first-stage in the radical-initiated reduction of the low-spin Fe(II) of the [Fe(Cys)$(CO)_2$(CN)] synthon to Fe(I) en route to H-cluster formation and installation in HydA1. This builds upon the prior work of Nicolet et al.[14] showing that the 5′-dA● radical generated by *Tm*HydE directly attacks the sulfur atom of 1,3-thiazolidine to form a new C5′−S bond. We now show a similar reaction occurs in HydE's interaction with syn-B, which we have previously shown to be a functional carrier of the organometallic [Fe^{II}(Cys)$(CO)_2$(CN)] precursor on path to hydrogenase activation.[16] Here the 5′-dA● radical reacts directly with the synthon's cysteine sulfur to form a C5′−S bond. This reinforces that point made by Nicolet et al.[14] that HydE is a member of very small family of rSAM enzymes in which the generated 5′-dA● radical does not drive hydrogen-atom abstraction, but instead performs another function, such as addition of the 5′-dA● radical to a double bond to generate a C−C bond.[29,30]

The further time evolution of the Fe(I) intermediate. We investigated the evolution of the HydE reaction with syn-B at longer times, obtaining EPR spectra (35 K observation temperature) of reaction mixtures quenched at 2 and 10 min (Figure 4A). The X-band CW EPR spectrum of the 2 min-reaction sample recorded at 35 K exhibits a rather complicated signal with at least two components (Figure S7), while at 10 min the EPR spectrum is dominated by a single new $S = 1/2$ signal with a **g** tensor of [g_1, g_2, g_3] = [2.098, 2.080, 2.005] (g_{iso}

https://dx.doi.org/10.1021/jacs.0c03802
J. Am. Chem. Soc. 2020, 142, 10841−10848

= 2.061) that is amenable for further pulse EPR interrogation. Although the central g_2 value is shifted appreciably relative to the 10 s-intermediate, the total span of g-values and its spin-relaxation properties (with the optimal signal acquired at 35 K), are similar to those of the 10 s-intermediate, suggesting that this species trapped at 10 min is also a low-spin Fe(I) species. The 10 min sample prepared with syn-B−^{13}CN shows only one ^{13}C hyperfine coupling ($A \approx 27$ MHz, Figure 4B), as well as the clear ^{13}C-split doublet presented at the g_3 position of the corresponding CW EPR spectrum (Figure S7), again indicating that at 10 min in the reaction the intermediate remains a mono-Fe(I) species with one CN^- ligand. However, in stark contrast to the 10 s-intermediate, the 10 min-species prepared with syn-B−$^{13}C_3$/^{15}N-Cys shows no sign of ^{13}C or ^{15}N couplings to the Fe(I) center. GC-MS of the reaction mixture shows the presence of $^{13}C_3$-labeled pyruvate (~100% isotope enriched, see the SI Methods), indicating that the cysteine C3−S bond has been cleaved. Thus, HydE is now shown responsible for the on-pathway reaction characterized in our prior work with syn-B in the full *in vitro* maturation experiment,[16] in which the Fe−S bond is retained while the entire C/N backbone of Cys is cleaved away, ultimately to be replaced by the serine-derived C−N−C bridgehead moiety.[17]

For the 10 min-species prepared with $^{13}C_{10}$-adenosine-labeled SAM, we observe a ~1.5 MHz ^{13}C hyperfine coupling (Figure 4B), showing that adenosine ^{13}C remains coupled to the Fe(I) center and indicating that the C5′−S bond remains intact at the 10 min time point. Although the ^{13}C5′ hyperfine value is smaller than that of 10 s-intermediate, this could be due to less spin-density delocalized to C5′ resulting from a possible geometric reorganization with the release of the C/N-backbone of Cys (see DFT in Figure S8). We also performed the full maturation reaction using $^{13}C_{10}$/$^{15}N_5$-adenosine-labeled SAM and characterized the resulting H_{ox} H-cluster signal by ENDOR (Figure S9), with no hyperfine couplings detected, showing that the ribose linkage must be released before or concomitant with the installation of the final C−N−C bridgehead.

DISCUSSION

Experimental characterization of the 10 s and 10 min species of the HydE syn-B unit reaction positions us for future experiments to determine how HydE, HydF, and HydA1 complete the biosynthesis of the $[2Fe]_H$-subcluster. In the meantime, we can speculate the following: the generation of Fe(I) centers by HydE should be a prerequisite for the formation of an Fe(I)Fe(I) dimer, of which there are a number of synthetic examples.[31−33] By comparing the geometric structure of the 10 min-species with the $[2Fe]_H$-subcluster of the H-cluster, we can envision a possible dimerization process (Figure 5) that is coupled to the installation of the serine-derived bridging $NH(CH_2)_2$. Probing this chemistry is our next experimental target using our combination of chemical isotope labeling, pulse EPR methods, and other spectroscopies.

In summary, by employing the synthetic syn-B complex in reaction time-dependent EPR experiments, we have established that the $[Fe^{II}(Cys)(CO)_2(CN)]$ HydG-reaction product, as donated by our synthetic carrier syn-B, is the substrate of the HydE enzyme. Our prior work shows this reaction is on pathway to H-cluster formation and activation of hydrogenase activity. This new work provides important new details of the enzymology of HydE, the second rSAM enzyme employed in the process. We show that HydE reduces the low-spin Fe(II) center of the synthon to generate a mononuclear low-spin Fe(I) intermediate via a radical-addition mechanism. The as-formed Fe(I) intermediate further evolves to release the C/N-containing fragment of Cys to form a mononuclear $[Fe^I(CO)_2(CN)S]$ species which is well suited to condense to a $[Fe^I_2(CO)_4(CN)_2S_2]$ center, reminiscent of the $Fe_2(CO)_6S_2$ species of Hieber and Gruber.[34] This compact inorganic species needs only the installation of the C−N−C bridgehead to complete the $[2Fe]_H$-subcluster. Therefore, this work reveals a new role for rSAM enzymes in formation of an unusual organometallic Fe(I) species and provides new direct experimental insights in the role played by HydE in the enzymatic assembly of the H-cluster.

METHODS

Preparation of syn-B Complex. Synthetic organometallic chemistry leading to the syn-B complexes employed in this work, including **syn-B**, **syn-B−^{13}CN**, **syn-B−$^{13}C_3$/^{15}N-Cys**, **syn-B-cysteamine** and **syn-B-selenocysteine**, was conducted by using glovebox and Schlenkline techniques. Detailed descriptions of syn-B synthesis are given in ref 16. The corresponding Fourier transform infrared (FT-IR) spectra as well as the electrospray ionization−mass spectrometry (ESI-MS) characterization are also provided by ref 16.

Expression and Purification of *Tm*HydE Enzyme. The plasmid used in this work is a C-terminal *strep*-tag II containing pET-21b(+) vector with a codon-optimized *Thermotoga maritima* hydE gene insert in which the three C-terminal cysteine (Cys) residues are mutated to serine residues (C311S/C319S/C321S). This mutant is chosen based on previous work by Nicolet et al.[14,19] which suggested that the semiconserved accessory Fe−S cluster has no reported function for the [FeFe]-hydrogenase H-cluster activity and provokes a local structural heterogeneity. Therefore, the *Tm*HydE enzyme employed in this work contains only the N-terminal rSAM [4Fe−4S] cluster, simplifying EPR assignments. We also confirmed that the wild-type *Tm*HydE enzyme generates the same mononuclear Fe(I) intermediate at 10 s (shown in Figure S10).

The plasmid was transformed into *E. coli* BL21(DE3) Δ*iscR* competent cell with kanamycin resistance. Cells were grown in Luria−Bertani broth containing 40 mg/L kanamycin, 100 mg/L ampicillin, 2 mM ammonium ferric citrate, 0.5% (w/v) glucose and 100 mM 3-(*N*-morpholino)propanesulfonic acid (MOPS, pH 7.8) at 28 °C to an $O.D._{600} \approx 0.4$. Then the cultures were pooled, transferred into the anaerobic chamber, and supplemented with 5 mM Cys and 10 mM fumarate. The pooled culture was stirred in the chamber for ca. 40 min to deplete the remaining oxygen in the solution, and protein expression was then induced by 0.25 mM isopropyl β-D-1-thiogalactopyranoside (IPTG). After ~22 h, cells were harvested by centrifugation (6000 rpm at 4 °C for 30 min), flash frozen in liquid nitrogen and stored at −80 °C.

For protein purification, cells were lysed in a HEPES buffer (buffer W, 50 mM HEPES, 150 mM KCl, pH 8.0) containing 1 × Bugbuster detergent solution (EMD Millipore), 25 U/mL benzonanse (EMD Millipore), 1 kU/mL rLysozyme (EMD Millipore), and one EDTA-free protease inhibitor cocktail tablet (Roche). The cell debris was removed by centrifugation (18 000 rpm at 4 °C for 30 min) and the clear supernatant was loaded to a 50 mL column volume of *strep*-tactin resin in a gravity column. The unbound protein fraction was removed by gravity-flowing through the resin and the resin was washed with 100 mL buffer W. The *Tm*HydE protein fraction was eluted by adding 100 mL buffer W containing 3 mM desthiobiotin. The dark protein fraction was collected. The as-eluted protein with the concentration of ~300 μM was aliquoted, flash frozen in liquid nitrogen, and stored at −80 °C.

EPR Sample Preparation. *Tm*HydE reaction mixtures were prepared anaerobically. First 100 μL of as-eluted *Tm*HydE (~300 μM) in a pH-buffered solution (50 mM HEPES, 150 mM KCl, pH 8.0) was incubated with 20 equiv of sodium dithionite (DTH) and 10 equiv of SAM for ~10 min. Then around 10 equiv of syn-B aqueous

https://dx.doi.org/10.1021/jacs.0c03802
J. Am. Chem. Soc. 2020, 142, 10841−10848

solution was added to initiate the reaction. After being allowed to react for set times, samples were frozen and stored in liquid N_2 for EPR characterization. We confirmed that the organometallic Fe(I) species can also be generated by *So*HydE (see Figure S11), but with faster kinetics compared to the thermophile *Tm*HydE.

■ ASSOCIATED CONTENT

Supporting Information

The Supporting Information is available free of charge at https://pubs.acs.org/doi/10.1021/jacs.0c03802.

Detailed experimental methods; DFT calculations of the Fe(I) intermediates generated through HydE reaction; LC-MS analysis of HydE reaction samples; similar Fe(I) intermediate generated by *So*HydE from *Shewanella oneidensis* (PDF)

■ AUTHOR INFORMATION

Corresponding Author

R. David Britt − *Department of Chemistry, University of California at Davis, Davis, California 95616, United States;* orcid.org/0000-0003-0889-8436; Email: rdbritt@ucdavis.edu

Authors

Lizhi Tao − *Department of Chemistry, University of California at Davis, Davis, California 95616, United States;* orcid.org/0000-0001-9921-2297

Scott A. Pattenaude − *School of Chemical Sciences, University of Illinois at Urbana−Champaign, Urbana, Illinois 61801, United States;* orcid.org/0000-0002-0564-2796

Sumedh Joshi − *Department of Chemistry, Texas A&M University, Texas 77842, United States;* orcid.org/0000-0002-0407-2920

Tadhg P. Begley − *Department of Chemistry, Texas A&M University, Texas 77842, United States;* orcid.org/0000-0001-5134-2623

Thomas B. Rauchfuss − *School of Chemical Sciences, University of Illinois at Urbana−Champaign, Urbana, Illinois 61801, United States;* orcid.org/0000-0003-2547-5128

Complete contact information is available at: https://pubs.acs.org/10.1021/jacs.0c03802

Notes

The authors declare no competing financial interest.

■ ACKNOWLEDGMENTS

We thank Dr. Lucas Li and Dr. Alexander Ulanov at the Roy J. Carver Biotechnology Center (University of Illinois Urbana−Champaign) for help with pyruvate detection and quantification. This work was supported by the National Institutes of Health (1R35GM126961-01 to R.D.B. and GM61153 to T.B.R.) and by Robert A. Welch Foundation (A-0034) and National Science Foundation (1905336 to T.P.B.).

■ REFERENCES

(1) Lubitz, W.; Ogata, H.; Rüdiger, O.; Reijerse, E. Hydrogenases. *Chem. Rev.* **2014**, *114* (8), 4081−4148.

(2) Peters, J. W.; Lanzilotta, W. N.; Lemon, B. J.; Seefeldt, L. C. X-ray crystal structure of the Fe-only hydrogenase (CpI) from *Clostridium pasteurianum* to 1.8 angstrom resolution. *Science* **1998**, *282* (5395), 1853−1858.

(3) Mulder, D. W.; Shepard, E. M.; Meuser, J. E.; Joshi, N.; King, P. W.; Posewitz, M. C.; Broderick, J. B.; Peters, J. W. Insights into [FeFe]-hydrogenase structure, mechanism, and maturation. *Structure* **2011**, *19* (8), 1038−1052.

(4) Mulder, D. W.; Boyd, E. S.; Sarma, R.; Lange, R. K.; Endrizzi, J. A.; Broderick, J. B.; Peters, J. W. Stepwise [FeFe]-hydrogenase H-cluster assembly revealed in the structure of $HydA^{\Delta EFG}$. *Nature* **2010**, *465* (7295), 248−251.

(5) Shepard, E. M.; Mus, F.; Betz, J. N.; Byer, A. S.; Duffus, B. R.; Peters, J. W.; Broderick, J. B. [FeFe]-hydrogenase maturation. *Biochemistry* **2014**, *53* (25), 4090−4104.

(6) Kuchenreuther, J. M.; Myers, W. K.; Stich, T. A.; George, S. J.; NejatyJahromy, Y.; Swartz, J. R.; Britt, R. D. A radical intermediate in tyrosine scission to the CO and CN^- ligands of FeFe Hydrogenase. *Science* **2013**, *342* (6157), 472−475.

(7) Kuchenreuther, J. M.; Myers, W. K.; Suess, D. L. M.; Stich, T. A.; Pelmenschikov, V.; Shiigi, S. A.; Cramer, S. P.; Swartz, J. R.; Britt, R. D.; George, S. J. The HydG enzyme generates an $Fe(CO)_2(CN)$ synthon in assembly of the FeFe hydrogenase H-cluster. *Science* **2014**, *343* (6169), 424−427.

(8) Suess, D. L. M.; Bürstel, I.; De La Paz, L.; Kuchenreuther, J. M.; Pham, C. C.; Cramer, S. P.; Swartz, J. R.; Britt, R. D. Cysteine as a ligand platform in the biosynthesis of the FeFe hydrogenase H cluster. *Proc. Natl. Acad. Sci. U. S. A.* **2015**, *112* (37), 11455−11460.

(9) Rao, G.; Tao, L.; Suess, D. L. M.; Britt, R. D. A [4Fe−4S]-Fe(CO)(CN)-l-cysteine intermediate is the first organometallic precursor in [FeFe] hydrogenase H-cluster bioassembly. *Nat. Chem.* **2018**, *10* (5), 555−560.

(10) Pagnier, A.; Martin, L.; Zeppieri, L.; Nicolet, Y.; Fontecilla-Camps, J. C. CO and CN^- syntheses by [FeFe]-hydrogenase maturase HydG are catalytically differentiated events. *Proc. Natl. Acad. Sci. U. S. A.* **2016**, *113* (1), 104−109.

(11) Shepard, E. M.; McGlynn, S. E.; Bueling, A. L.; Grady-Smith, C. S.; George, S. J.; Winslow, M. A.; Cramer, S. P.; Peters, J. W.; Broderick, J. B. Synthesis of the 2Fe subcluster of the [FeFe]-hydrogenase H cluster on the HydF scaffold. *Proc. Natl. Acad. Sci. U. S. A.* **2010**, *107* (23), 10448−10453.

(12) Caserta, G.; Pecqueur, L.; Adamska-Venkatesh, A.; Papini, C.; Roy, S.; Artero, V.; Atta, M.; Reijerse, E.; Lubitz, W.; Fontecave, M. Structural and functional characterization of the hydrogenase-maturation HydF protein. *Nat. Chem. Biol.* **2017**, *13* (7), 779−784.

(13) Betz, J. N.; Boswell, N. W.; Fugate, C. J.; Holliday, G. L.; Akiva, E.; Scott, A. G.; Babbitt, P. C.; Peters, J. W.; Shepard, E. M.; Broderick, J. B. [FeFe]-hydrogenase maturation: insights into the role HydE plays in dithiomethylamine biosynthesis. *Biochemistry* **2015**, *54* (9), 1807−1818.

(14) Rohac, R.; Amara, P.; Benjdia, A.; Martin, L.; Ruffié, P.; Favier, A.; Berteau, O.; Mouesca, J.-M.; Fontecilla-Camps, J. C.; Nicolet, Y. Carbon−sulfur bond-forming reaction catalysed by the radical SAM enzyme HydE. *Nat. Chem.* **2016**, *8* (5), 491−500.

(15) Kuchenreuther, J. M.; Britt, R. D.; Swartz, J. R. New insights into [FeFe] hydrogenase activation and maturase function. *PLoS One* **2012**, *7* (9), No. e45850.

(16) Rao, G.; Pattenaude, S. A.; Alwan, K.; Blackburn, N. J.; Britt, R. D.; Rauchfuss, T. B. The binuclear cluster of [FeFe] hydrogenase is formed with sulfur donated by cysteine of an $[Fe(Cys)(CO)_2(CN)]$ organometallic precursor. *Proc. Natl. Acad. Sci. U. S. A.* **2019**, *116* (42), 20850−20855.

(17) Rao, G.; Tao, L.; Britt, R. D. Serine is the molecular source of the $NH(CH_2)_2$ bridgehead moiety of the *in vitro* assembled [FeFe] hydrogenase H-cluster. *Chem. Sci.* **2020**, *11*, 1241−1247.

(18) Broderick, J. B.; Duffus, B. R.; Duschene, K. S.; Shepard, E. M. Radical *S*-adenosylmethionine enzymes. *Chem. Rev.* **2014**, *114* (8), 4229−4317.

(19) Nicolet, Y.; Rubach, J. K.; Posewitz, M. C.; Amara, P.; Mathevon, C.; Atta, M.; Fontecave, M.; Fontecilla-Camps, J. C. X-ray structure of the [FeFe]-Hydrogenase maturase HydE from *Thermotoga maritima*. *J. Biol. Chem.* **2008**, *283* (27), 18861−18872.

(20) Rubach, J. K.; Brazzolotto, X.; Gaillard, J.; Fontecave, M. Biochemical characterization of the HydE and HydG iron-only

hydrogenase maturation enzymes from *Thermatoga maritima*. *FEBS Lett.* **2005**, *579* (22), 5055−5060.
(21) Sayler, R. I.; Stich, T. A.; Joshi, S.; Cooper, N.; Shaw, J. T.; Begley, T. P.; Tantillo, D. J.; Britt, R. D. Trapping and electron paramagnetic resonance characterization of the 5′-dAdo• radical in a radical *S*-adenosyl methionine enzyme reaction with a non-native substrate. *ACS Cent. Sci.* **2019**, *5* (11), 1777−1785.
(22) Böck, A.; King, P. W.; Blokesch, M.; Posewitz, M. C. Maturation of hydrogenases. In *Advances in Microbial Physiology*; Poole, R. K., Ed.; Academic Press: New York, 2006; Vol. *51*, pp 1−225.
(23) Palmer, G. Electron paramagnetic resonance of metalloproteins. In *Physical Methods in Bioinorganic Chemistry: Spectroscopy and Magnetism*; Lawrence Que, J., Ed.; University Science Books: Sausalito, CA, 2000.
(24) Hendrich, M. P.; Debrunner, P. G. Integer-spin electron paramagnetic resonance of iron proteins. *Biophys. J.* **1989**, *56* (3), 489−506.
(25) Zoppellaro, G.; Bren, K. L.; Ensign, A. A.; Harbitz, E.; Kaur, R.; Hersleth, H.-P.; Ryde, U.; Hederstedt, L.; Andersson, K. K. Studies of ferric heme proteins with highly anisotropic/highly axial low spin (S = 1/2) electron paramagnetic resonance signals with bis-Histidine and histidine-methionine axial iron coordination. *Biopolymers* **2009**, *91* (12), 1064−1082.
(26) Myers, W. K.; Stich, T. A.; Suess, D. L. M.; Kuchenreuther, J. M.; Swartz, J. R.; Britt, R. D. The cyanide ligands of [FeFe] hydrogenase: pulse EPR studies of ^{13}C and ^{15}N-labeled H-cluster. *J. Am. Chem. Soc.* **2014**, *136* (35), 12237−12240.
(27) Citek, C.; Oyala, P. H.; Peters, J. C. Mononuclear Fe(I) and Fe(II) acetylene adducts and their reductive protonation to terminal Fe(IV) and Fe(V) carbynes. *J. Am. Chem. Soc.* **2019**, *141* (38), 15211−15221.
(28) Horitani, M.; Shisler, K.; Broderick, W. E.; Hutcheson, R. U.; Duschene, K. S.; Marts, A. R.; Hoffman, B. M.; Broderick, J. B. Radical SAM catalysis via an organometallic intermediate with an Fe-[5′-C]-deoxyadenosyl bond. *Science* **2016**, *352* (6287), 822−825.
(29) Mahanta, N.; Fedoseyenko, D.; Dairi, T.; Begley, T. P. Menaquinone biosynthesis: formation of aminofutalosine requires a unique radical SAM enzyme. *J. Am. Chem. Soc.* **2013**, *135* (41), 15318−15321.
(30) Sato, S.; Kudo, F.; Rohmer, M.; Eguchi, T. Characterization of radical SAM adenosylhopane synthase, HpnH, which catalyzes the 5′-deoxyadenosyl radical addition to diploptene in the biosynthesis of C35 bacteriohopanepolyols. *Angew. Chem., Int. Ed.* **2020**, *59* (1), 237−241.
(31) Gilbert-Wilson, R.; Siebel, J. F.; Adamska-Venkatesh, A.; Pham, C. C.; Reijerse, E.; Wang, H.; Cramer, S. P.; Lubitz, W.; Rauchfuss, T. B. Spectroscopic investigations of [FeFe] hydrogenase maturated with $[^{57}Fe_2(adt)(CN)_2(CO)_4]^{2-}$. *J. Am. Chem. Soc.* **2015**, *137* (28), 8998−9005.
(32) Li, Y.; Rauchfuss, T. B. Synthesis of diiron(I) dithiolato carbonyl complexes. *Chem. Rev.* **2016**, *116* (12), 7043−7077.
(33) Berggren, G.; Adamska, A.; Lambertz, C.; Simmons, T. R.; Esselborn, J.; Atta, M.; Gambarelli, S.; Mouesca, J. M.; Reijerse, E.; Lubitz, W.; Happe, T.; Artero, V.; Fontecave, M. Biomimetic assembly and activation of [FeFe]-hydrogenases. *Nature* **2013**, *499* (7456), 66−69.
(34) Hieber, W.; Gruber, J. Zur Kenntnis der Eisencarbonylchalkogenide. *Z. Anorg. Allg. Chem.* **1958**, *296* (1−6), 91−103.

https://dx.doi.org/10.1021/jacs.0c03802
J. Am. Chem. Soc. 2020, 142, 10841−10848